

Statins Increase p21 through Inhibition of Histone Deacetylase Activity and Release of Promoter-Associated HDAC1/2

Yi-Chu Lin,¹ Jung-Hsin Lin,^{2,3,4} Chia-Wei Chou,¹ Yu-Fan Chang,¹ Shu-Hao Yeh,² and Ching-Chow Chen¹

¹Department of Pharmacology and ²School of Pharmacy, College of Medicine, National Taiwan University; ³Division of Mechanics, Research Center for Applied Sciences and ⁴Institute of Biomedical Science, Academia Sinica, Taipei, Taiwan

Abstract

Statins are 3-hydroxy-3-methylglutaryl-CoA reductase inhibitors broadly used for the control of hypercholesterolemia. Recently, they are reported to have beneficial effects on certain cancers. In this study, we show that statins inhibited the histone deacetylase (HDAC) activity and increased the accumulation of acetylated histone-H3 and the expression of p21^{WAF/CIP} in human cancer cells. Computational modeling showed the direct interaction of the carboxylic acid moiety of statins with the catalytic site of HDAC2. In the subsequent enzymatic assay, it was shown that lovastatin inhibited HDAC2 activity competitively with a K_i value of 31.6 $\mu\text{mol/L}$. Sp1 but not p53 sites were found to be the statins-responsive element shown by p21 luciferase-promoter assays. DNA affinity protein binding assay and chromatin immunoprecipitation assay showed the dissociation of HDAC1/2 and association of CBP, leading to the histone-H3 acetylation on the Sp1 sites of p21 promoter. *In vitro* cell proliferation and *in vivo* tumor growth were both inhibited by statins. These results suggest a novel mechanism for statins through abrogation of the HDAC activity and promoter histone-H3 acetylation to regulate p21 expression. Therefore, statins might serve as novel HDAC inhibitors for cancer therapy and chemoprevention. [Cancer Res 2008;68(7):2375–83]

Introduction

Statins can reduce serum cholesterol levels by competitively inhibiting 3-hydroxy-3-methylglutaryl-CoA (HMG-CoA) reductase, the rate-limiting enzyme in the synthesis of mevalonate (the fatty acid intermediate in cholesterol biosynthesis). This effect contributes to their decrease in the incidence of cardiovascular and cerebrovascular disorders and their remarkable prevention of cardiovascular disease (CVD; ref. 1). By inhibiting the biosynthesis of mevalonate, statins also inhibit the formation of downstream lipid isoprenoid intermediates, such as farnesyl PPI (FPP) and geranylgeranyl PPI (GGPP). The isoprenoids are lipid moieties that are added to various proteins, including Ras, Rho, and Rac of small G proteins during posttranslational modification (prenylation), and anchor these proteins to the cell membrane (2). Statins have an established record of human safety and efficacy in CVD prevention and also show promise for cancer prevention in observational,

preclinical, and certain aspects of randomized controlled studies (3). These studies have focused primarily on the malignancy of colorectal, breast, prostate, and melanocyte and indicate that statins are one of the most promising classes of agents currently available for testing in cancer prevention. Statins have been reported to inhibit proliferation by down-regulating CDK2 activity or up-regulating p21 expression. Simvastatin inhibited high glucose-induced mesangial cell proliferation through preventing geranylgeranylation of Rho GTPase by reversing p21 down-regulation (4). However, transcriptional regulation of p21 expression in a p53-independent manner by lovastatin has also been reported (5). Therefore, understanding the molecular mechanism will help develop selective-targeting approaches for statins to prevent cancer and several other aging-related diseases (for example, neurodegenerative disorders; ref. 3).

The acetylation of lysine residues on histones H3 and H4 represent the active or open state of chromatin, which allow various transcription factors access to the promoters of target genes. In contrast, deacetylation of lysine residues results in chromatin compaction and transcriptional repression (6). This posttranslational modification is maintained by a dynamic balance between the activities of histone acetyltransferases and histone deacetylases (HDAC). Human tumors are frequently characterized with an overall loss of acetylation at histone that is considered as universal epigenetic markers for malignant transformation (7). Overexpression of HDACs is observed in human cancer tissues from a range of organs, such as stomach, colon, and breast (8). Most studies to date have focused on the aberrant recruitment of HDACs to promoters through physical association with oncogenic DNA-binding fusion proteins. For example, the oncogenic PML-RAR α , PLZF-RAR α , and AML1-ETO fusion proteins recruit HDAC-containing repressor complexes to repress the genes required for myeloid differentiation, thus induce acute promyelocytic leukemia and acute myeloid leukemia (9). Yet, the exact mechanism of how HDACs are recruited to functional genes is still unknown. Nevertheless, restoration of a "normal" epigenetic state by HDAC inhibitors could be a promising approach for cancer therapy (7).

The HDAC inhibitors are categorized into four groups: short-chain fatty acids, hydroxamic acids, cyclic tetrapeptides, and benzamides (8). Among them, trichostatin A (TSA), butyrate, vaproic acid (VPA), and MS275 have been shown to induce the expression of cyclin-dependent kinase inhibitors, such as p21, to activate the death receptor-mediated apoptotic pathway and to change the expression of genes involved in angiogenesis and metastasis (10). TSA and suberoylanilide hydroxamic acid (SAHA), the most potent HDAC inhibitors, both contain hydroxamic acid functional group. Statins in acid form possessing a carboxylic acid-containing long chain have a very similar structure to TSA and SAHA (Supplementary Fig. S1), and we found that statins induce hyperacetylation of H3. Therefore, we test the hypothesis that

Note: Supplementary data for this article are available at Cancer Research Online (<http://cancerres.aacrjournals.org/>).

Requests for reprints: Ching-Chow Chen, Department of Pharmacology, College of Medicine, National Taiwan University, No. 1, Jen-Ai Road, Section 1, Taipei 10018, Taiwan. Phone: 886-2-23123456, ext. 8321; Fax: 886-2-23947833; E-mail: chingchowchen@ntu.edu.tw.

©2008 American Association for Cancer Research.
doi:10.1158/0008-5472.CAN-07-5807

statins act as HDAC inhibitors. Molecular modeling supported this notion that the carboxylic acid moiety of lovastatin chelated the catalytic site of the human HDAC2, similar to the way that TSA does. Our *in vitro* experiments revealed that statins indeed inhibit the HDAC activity and increase the histone acetylation in human cancer cells. Furthermore, statins induced p21 expression through dissociation of HDAC1/2 and association of CBP, leading to histone acetylation on the Sp1 sites of p21 promoter. Both *in vitro* cell proliferation and *in vivo* xenograft model showed the antitumor activity of statins. These findings show a novel function of statins and provide a new thought for cancer therapy and chemoprevention.

Materials and Methods

Materials. Lovastatin was from Lotus Pharmaceutical Co. Atovastatin, pravastatin, and simvastatin were obtained from Synpac Kingdom Pharmaceutical Co. Fluvastatin was a gift from Novartis. TSA and VPA were obtained from Sigma. The human wild-type p21 promoter-luciferase fusion plasmid pWWP-Luc and a series of plasmids of mutant Sp1 were kindly donated by Dr. T Sakai (University of Tokyo). The antibodies specific for p21, p53, HDAC1, HDAC3, and β -actin were purchased from Santa Cruz Biotechnology. Anti-Ac-histone H3, HDAC2, and Sp1 antibodies were obtained from Upstate.

Cell culture. A549 human lung carcinoma cells from American Type Culture Collection (ATCC) and HCT-116, HCT-116 p53^{-/-} human colon carcinoma cells (from Van Dyke MW, M.D. Anderson) were cultured in DMEM supplemented with 10% fetal bovine serum; NCI-H292 human lung carcinoma cells and AGS human gastric carcinoma cells from ATCC were maintained in RPMI supplemented with 10% FCS.

HDAC activity assay. The HDAC activity was determined using the Fluor-de-Lys HDAC activity assay kit (Biomol). Incubations were performed at 37°C with cell extracts, statins, or TSA, and HDAC reaction was initiated by the addition of Fluor-de-Lys substrate. After adequate minutes, Fluor-de-Lys Developer was added, and the mixture was incubated for another 10 min at room temperature. Fluorescence was measured using a fluorimetric reader with excitation at 360 nm and emission at 460 nm. The HDAC activity was expressed as arbitrary fluorescence units. For HDAC2 enzymatic assay, HDAC2 recombinant protein was incubated with adequate concentration of acetylated substrate in assay buffer containing or lacking lovastatin. The K_i values for the test compounds were calculated from Lineweaver-Burk plots.

Immunoprecipitation. Cell extracts were immunoprecipitated by using antibodies against HDAC1, HDAC2, and HDAC3. Immune complexes were then incubated with proteinase A/G agarose beads for 1 h. All immunoprecipitates were washed thrice with PBS buffer before the HDAC activity assay.

Homology modeling. The sequence alignment between human HDAC2 and histone deacetylase-like protein (HDLP) was determined by the multiple sequence alignment between human class I HDACs (HDAC1, HDAC2, HDAC3, and HDAC8) and HDLP (11). The crystal water molecules within 30 Å from the center of mass of protein and the cocrystallized inhibitor of HDLP, TSA, were included in the template structure. The homology models generated were optimized by molecular dynamics module implemented in MODELLER 9.1 (12). The one with the lowest energy score was chosen as the final model, and then its quality was further checked with PROCHECK (13, 14).

Assignment of protonation states and partial charges. For the HDAC2 homology model, the hydrogen atoms were added by PDB2PQR (15) and the protonation states of residues around active site were carefully inspected (16). The histidine residues 141 and 142 were assigned to HID, and the histidine residue 179 was assigned to HIE. The aspartic acid residues 175, 177, 182, and 265 were assigned to be deprotonated, whereas the tyrosine residue 304 was set to be protonated. The ligand atomic charges were calculated by Gaussian98 program (Gaussian, Inc.) at the HF/6-31G* level and then fitted by the RESP method. The atomic charges

on protein were generated by LEaP module of the AMBER 9.0 suite AMBER 9 (University of California-San Francisco).

Molecular docking. The docking simulations were performed by both AutoDock 3.0.5 (17) and MEDock (18). The grid center was set at the center of the protein, and the grid box size was set to 90 × 90 × 90 points with a grid spacing of 0.375 Å. The grid box was set to be large enough to include the entire active site. The rotatable bonds of ligands were checked manually, and the ones without resonance were allowed to rotate. The charges of nonpolar hydrogens in the ligands were merged to the charge of carbons that they attached. The charge of zinc was set to +2, and its van der Waals variables were taken from Stote et al. (19). In the docking simulation, 100 runs were performed for AutoDock and MEDock. The Lamarckian genetic algorithm implemented in AutoDock was used for searching the global minimum, whereas a novel information theory-based evolutionary algorithm was implemented in MEDock as the search algorithm. The maximum number of energy evaluations and maximum number of generation were set to 10⁷ and 2.5 × 10⁴, respectively. The other docking variables were set as default values.

Western blot analysis. After treatment with statins, total cell lysates or nuclear extracts were prepared and subjected to SDS-PAGE using adequate percentage polyacrylamide gels.

Reverse transcription-PCR. Total RNA was isolated from A549 cell using Trizol reagent (Life Technology). Reverse transcription reaction was performed using 2 µg of total RNA, reverse transcribed into cDNA using oligo dT primer, and then amplified 30 cycles using two oligonucleotide primers derived from published p21 or β -actin sequence, including 5'-CAGAGGAGGCGCCATGTCAG-3' and 5'-CCTGTGGCGGATTAGG G-3' (p21) or 5'-TGACGGGGTACCCACACTGTGCCCATCTA-3' and 5'-CTAGA AGCATTTGCGGGGACGATGGAGGG-3' (β -actin). The PCR products were subjected to 1.5% agarose gel electrophoresis.

RNA protease assay. Total RNA was extracted from A549 cells with statins treatment by using TRIZOL reagent (Invitrogen). A RiboQuant multi-probe RNase protection assay (RPA) was performed with the hCC-2 biotin label probe set containing p130, Rb, p107, p53, p57, p27, p21, p19, p18, p16, p14/15, L32, and glyceraldehyde-3-phosphate dehydrogenase (GAPDH; BD Pharmingen). The probes were hybridized with 10 µg of RNA isolated from A549 cells. Samples were then digested with RNase to remove single-stranded RNA. Remaining probes were resolved on denaturing 5% polyacrylamide gels.

Transient transfection and luciferase activity assay. The vectors (pWWP and its serial mutant plasmids) were transiently transfected into A549 cells with Arrestin transfection reagent. Briefly, 2 µg of plasmid DNA, 1 µg of β -gal, and 3 µL transfection reagents were mixed, and the transfection protocol was carried out according to the manufacturer's instructions (Promega). Six hours after transfection, the cells were cultured in normal complete medium for another 16 h. The transfected cells with or without statin treatment were subjected to luciferase assay. Luciferase activities were normalized with the amount of protein in cell lysates.

Chromatin immunoprecipitation assay. Chromatin immunoprecipitation assay (ChIP) analysis was performed as described (20). Immunoprecipitated DNA was purified, resuspended in H₂O, and subjected to PCR. To amplify the regions p21 promoter, PCR was performed with the following pairs of primers: 5'-ACCAACGAGCGGAGGGACT-3' and 5'-CCGGCTCCACAA GGAAGTGA-3'. PCR products were then resolved by 1.5% agarose-ethidium bromide gel electrophoresis and visualized by UV.

DNA affinity protein binding assay. Oligonucleotides corresponding to the consensus sequences of Sp1 (5'-AGC TTGGAAATTCGGA-3') and (5'-TTCCGGAATTTCCAAGCT-3') of the human p21 promoter were synthesized, annealed, and end labeled with biotin.

Cell proliferation. For growth inhibition analysis, A549 cells were seeded at density of 1 × 10⁵ cells per well in six-well dishes. A solution containing various statins or TSA in DMSO was added in each dish after the seeding. The number of viable cells was counted for 3 d.

Flow cytometry. Cell cycle was determined by flow cytometry using a propidium iodide stain buffer and analyzed on a BD FACSCalibur cytometer with Cellquest software.

Animal xenograft assay. Female BALB/c nude mice (4–6 wk old) were injected with 10^7 A549 cells (suspended in 0.1 mL PBS and mixed with 0.1 mL Matrigel) in the rear left flank. Two weeks after administration, 100 to 200 mm³ tumors were apparent on all mice. At this time, animals were divided into two groups ($n = 6$) and orally received either control vehicle (soy oil) or lovastatin (20 mg/kg/d) suspended in soy oil. Mice were treated everyday for 30 d with lovastatin or control vehicle, and tumor growth was measured twice per week with calipers. Tumor volume (V) was calculated using the formula, V (mm³) = $0.52(ab^2)$, where a is length and b is width of the tumor (20).

Statistical analysis. All results are presented as mean \pm SE. The two-tailed Student's t test was used to calculate the statistical significance between groups.

Results

Statins inhibit HDAC activity and induce histone acetylation. A number of structurally diverse natural and synthetic compounds, such as TSA and SAHA, have been reported as HDAC inhibitors (Supplementary Fig. S1A). These compounds consist of a hydrophobic scaffold (benzyl group) with a spacer (aliphatic group) attaching to a functional group (hydroxamic acid) which can interact with zinc ion in the active site pocket (8, 10). Statins in acid form (open ring) possess a carboxylic acid-containing aliphatic group similar to the structure of TSA and SAHA (Supplementary Fig. S1B). To determine whether statins can inhibit HDAC, computational modeling of the HDAC2–statins interactions was conducted and the changes of HDAC activity caused by statins were examined *in vitro*. As shown in Fig. 1A, various statins (lovastatin, simvastatin, pravastatin, fluvastatin, and atorvastatin) at 10 μ mol/L inhibited the activity of HDACs in A549 nuclear extracts; TSA was a positive control. The dose-dependent inhibition of HDAC activity by lovastatin was seen (Supplementary Fig. S2). To assess whether HDAC inhibition by statins indeed leads to increase in histone acetylation, the level of acetylated histone-H3 was analyzed. As shown in Fig. 1B, acetylated histone-H3 was increased after treatment with 30 μ mol/L statins. To compare the effect of lovastatin with TSA and VPA, different concentrations of TSA or VPA or 30 μ mol/L lovastatin were used. The accumulation of global acetylated histone-H3 was seen after treatment with TSA from 0.125 to 1 μ mol/L or VPA from 1 to 5 mmol/L. There is a dramatic increase of acetylated histone-H3 by TSA from 0.5 to 1 μ mol/L (Fig. 1C). The extent of histone-H3 acetylation induced by 30 μ mol/L lovastatin is comparable with that of 0.5 μ mol/L TSA or 5 mmol/L VPA. To test whether statins affect the protein level of HDAC, the expression of class I HDACs was examined. The protein levels of HDAC1, HDAC2, and HDAC3 were not changed after statins or TSA treatment (Fig. 1D), demonstrating that inhibition of HDAC activity, but not HDAC expression, is responsible for the accumulation of acetylated histone-H3 after statins treatment.

Computational modeling of the interaction between lovastatin and human HDAC2. To consolidate the hypothesis whether there are substantial interactions between lovastatin and HDAC2, homology modeling and docking simulations were conducted. Docking of TSA into the HDAC2 homology model was first performed as a control. As shown in Fig. 2A, TSA inserted its long aliphatic chain into the tube-like pocket of HDAC2 and interacted with the zinc ion and active site residues of HDAC2 through its hydroxamic acid at one end of the aliphatic chain. This binding mode follows very similar pattern to the interaction of TSA and a bacterial HDLP (21). In the docking of lovastatin, two major binding modes were observed. In one binding mode, lovastatin was able to bind HDAC2 at an adjacent pocket (with a predicted K_i value of

0.53 nmol/L) near the active site (Fig. 2B), whereas in the other binding mode, lovastatin extends its long chain into the active site (with a predicted K_i value of 7.65 nmol/L) with the carboxylate group coordinating with zinc (Fig. 2C).

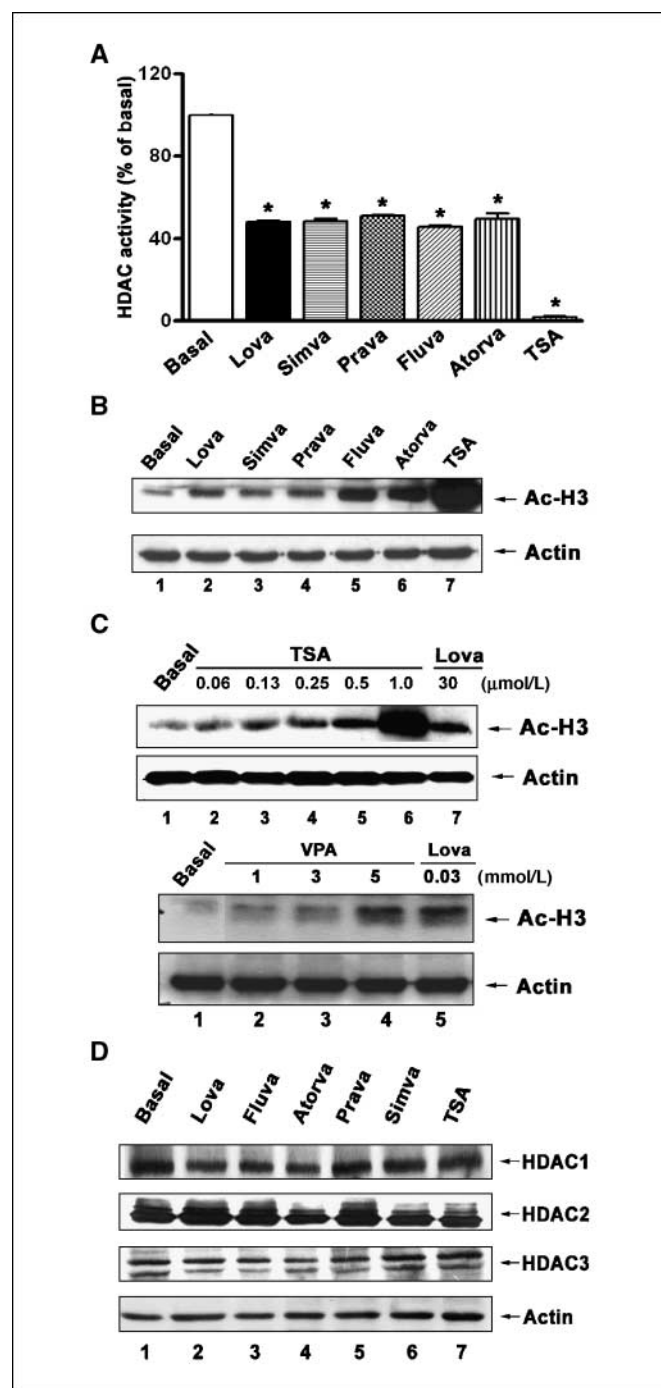


Figure 1. Inhibition of the HDAC activity and accumulation of histone-H3 acetylation by statins. **A**, nuclear HDAC activity in A549 cells was determined in the presence of 10 μ mol/L statins or 1 μ mol/L TSA using the HDAC activity assay kit as described in Materials and Methods. Columns, mean of three independent experiments performed in triplicate; bars, SE. *, $P < 0.05$ compared with basal. **B–D**, A549 cells were treated with 30 μ mol/L statins and different doses of TSA or VPA for 16 h, and then whole-cell lysates were prepared and subjected to Western blotting using antibody against acetyl histone-H3 or actin or HDAC1, HDAC2, and HDAC3.

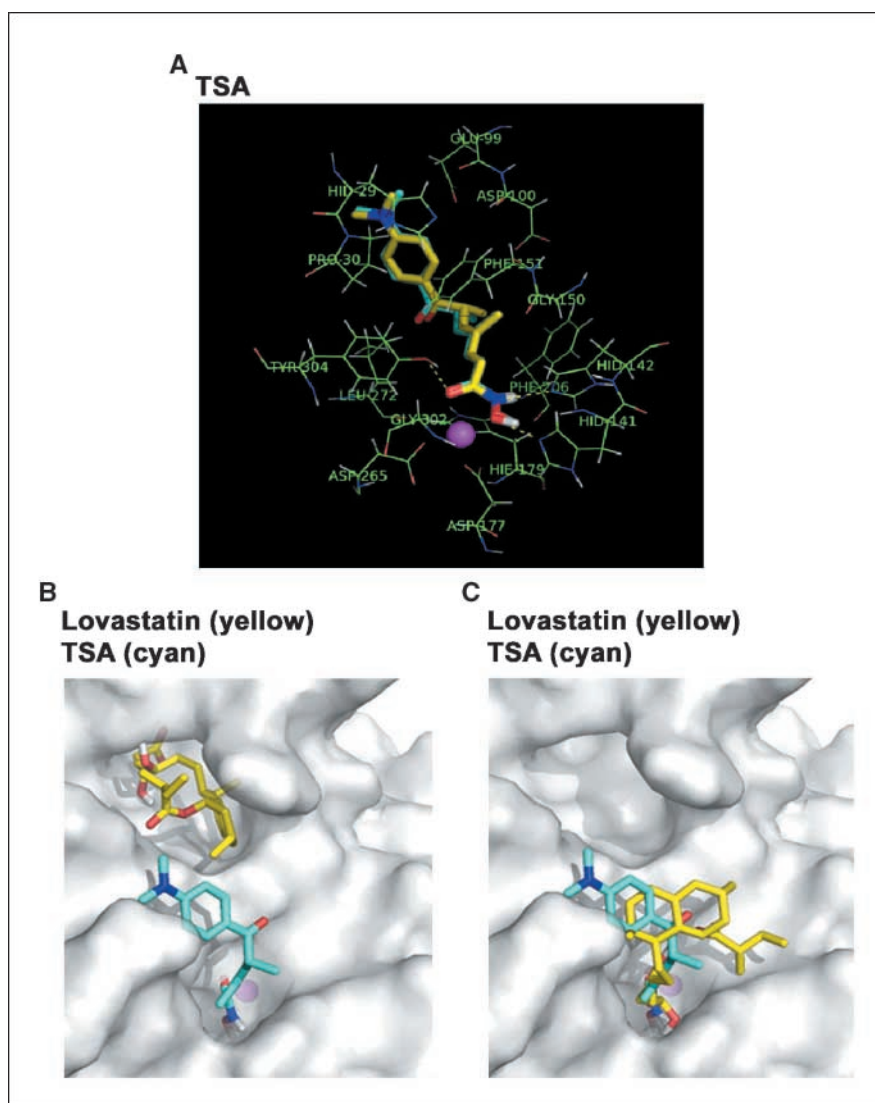


Figure 2. The predicted binding modes of HDAC2 and lovastatin. *A*, molecular modeling of the interactions between TSA and HDAC2. *Green lines*, residues within 4 Å from the mapped TSA in HDAC2; *magenta sphere*, zinc atom; *cyan*, mapped TSA; *yellow*, best docking model of TSA; *yellow dash lines*, hydrogen bonds that form between HDAC2 and TSA. *B*, the best docking model of lovastatin to HDAC2. *Magenta sphere*, zinc atom; *cyan*, mapped TSA; *yellow*, best docking model of lovastatin. Lovastatin was bound to the adjacent pocket near the active site. *C*, the other major binding mode of lovastatin to HDAC2. *Magenta sphere*, zinc atom; *cyan*, mapped TSA; *yellow*, best docking model of lovastatin. The lovastatin was bound into the active site of HDAC2.

Inhibition of HDAC activity by lovastatin. To gain a better understanding of lovastatin on HDAC inhibition, the kinetic variables (K_m and K_i values) were calculated according to the Lineweaver-Burk plot ($1/v$ versus $1/[substrate]$). As shown in Fig. 3A, K_m value was $57.6 \mu\text{mol/L}$ and K_i value was $31.6 \mu\text{mol/L}$. The Lineweaver-Burk plot showed that all the lines intersect at the same point on the $1/v$ axis in the absence or presence of lovastatin, demonstrating a competitive inhibition of lovastatin on HDAC2. The K_m value for TSA was $128 \mu\text{mol/L}$, and the K_i value was 0.3 nmol/L (data not shown). Because HDAC inhibitors might display distinct selectivity against different isoenzymes, which isoform was inhibited by statins was further examined. HDAC1, HDAC2, or HDAC3 was immunoprecipitated, and lovastatin showed the inhibition on these isoforms (Fig. 3B). To examine whether statins are broad HDAC inhibitors, cell lysates from several cancer cell lines, including lung cells A549 and NCI, gastric cells AGS, and colon cells HCT116, were used to measure the HDAC activity. Lovastatin at $30 \mu\text{mol/L}$ inhibited HDAC activity in all malignant cells (Fig. 3C) but had no effect on benign human umbilical vascular endothelial cell (data not shown).

Statins increased the protein and mRNA expressions of p21. Hyperacetylation of histones by HDAC inhibitors have been reported to activate tumor suppressor genes and repress oncogenes (8). To investigate the biological events aroused by statins, expression of cell cycle-related genes was examined by RPA. Statins and TSA increased p21 mRNA expression without increase in p53 mRNA (Fig. 4A). The increase in p21 mRNA was confirmed by reverse transcription-PCR (RT-PCR) and Western blotting (Fig. 4B and C, top). A dose-dependent increase of p21 expression by TSA and VPA was seen (Fig. 4C, middle and bottom). The p21 induction by $0.5 \mu\text{mol/L}$ TSA is comparable with that by $1 \mu\text{mol/L}$, although the extent of global histone-H3 acetylation is dramatically increased at $1 \mu\text{mol/L}$ (Fig. 4C, middle and Fig. 1C, top). The promoter activity using wild-type p21 promoter-luciferase plasmid (WWP-Luc) was also activated by statins and TSA (Fig. 4D).

Analysis of the statins responsive elements on the p21 promoter. To identify which of the *cis*-acting element is responsible for the statins-induced p21 expression, a series of p21 promoter-luciferase reporters were used, including the 2,326-bp full-length (pWWP), truncated (pWWP-delp53), and mutant forms

(pWP101-mtSp1-3, pWP101-mtSp1-4, and pWP101-mtSp1-5,6; Fig. 5A). The induction of p21 promoter activity by lovastatin or TSA was observed. Deletion of p53 had no effect on the lovastatin-induced or TSA-induced p21 promoter activity. By comparing the pWP101-mtSp1-3, pWP101-mtSp1-4, or pWP101-mtSp1-5,6 with pWWP, it was clear that promoter activity was strongly diminished when Sp1-3, Sp1-4, or Sp1-5,6 site was mutated. The statins-induced p21 expression was seen in both HCT116 wild-type and p53^{-/-} cells (Fig. 5B), and p53 expression was not affected by statins (data not shown).

The interaction between HDAC and Sp1/Sp3 after treatment with statins. Because Sp1 elements are important for statin-induced p21 expression, DNA affinity protein binding assay (DAPA) using biotin-labeled oligonucleotides covering Sp1-3 to Sp1-6 sites on p21 promoter was performed. Sp1 and Sp3 were both bound to Sp1 sites. However, the occupancy of Sp1 or Sp3 on the p21 promoter did not change after treatment with lovastatin or TSA. HDAC1 and HDAC2 were also bound to Sp1 sites in the basal state; however, these bindings disappeared or decreased after treatment with lovastatin or TSA (Fig. 5C, lanes 2 and 3). To examine the *in vivo* binding of Sp1, HDAC1, and HDAC2 to the p21 promoter, ChIP assay was performed. Consistent with the results of DAPA, the *in vivo* binding of Sp1 was not changed by lovastatin or TSA. However, dissociation of HDAC1/2 and association of CBP to the p21 promoter covering Sp1 sites were seen after treatment with lovastatin or TSA (Fig. 5D). To investigate whether the release of HDAC1/2 and recruitment of CBP increased histone acetylation on the p21 promoter, the binding of acetylated histone-H3 was further examined. The increased binding of histone-H3 acetylation to the p21 promoter was seen in the presence of lovastatin or TSA (Fig. 5D). These results showed that lovastatin induced release of the bound HDAC1/2 from the histone-DNA complex at Sp1 sites on the p21 promoter.

Statins inhibited cell proliferation and tumor growth of lung cancer xenograft. To investigate the anticancer potential of statins, *in vitro* cell proliferation and *in vivo* tumor growth were evaluated. 3-(4,5-Dimethylthiazol-2-yl)-2,5-diphenyltetrazolium bromide (MTT) assay examines the growth of cancer cells, and flow cytometry analyzes the cell cycle progression. Cell growth was inhibited by statins or TSA (Fig. 6A). The percentage of G₀-G₁ phase was increased in cells treated with statins, suggesting the arrest at G₁ phase (Fig. 6B). The *in vivo* tumor growth was assessed by xenograft model using nude mice, and mice had a smaller tumor volume and tumor weight after p.o. administration of lovastatin (20 mg/kg/d) for 45 days (Fig. 6C and D). The expression of p21 protein and histone-H3 acetylation in the excised tumors was also examined and was elevated from lovastatin-treated mice (Fig. 6D).

Discussion

Epidemiologic data have shown the correlation between statins and a decrease in cancer incidence. The anticancer effect of statins has attributed to the increase in apoptosis, the suppression of angiogenesis, and the alteration of invasion and metastatic potential (22). However, exact mechanism of their anticancer effect remains to be defined. In this study, we found statins inhibit the HDAC activity, resulting in the increase of global histone-H3 acetylation. Moreover, statins elicit p21 expression and histone-H3 acetylation on the p21 promoter by shifting the promoter occupancy from HDAC to CBP. *In vitro* and *in vivo* studies also

showed the effectiveness of statins to inhibit cell proliferation, cell cycle progression, and tumor formation. These results are encouraging and strengthen the concept that statins are promising agent for cancer therapy and prevention.

Inhibiting the biosynthesis of mevalonate, statins reduce the formation of FPP and GGPP. Posttranslational prenylation of Ras by FPP or Rho by GGPP is essential for the translocation of these small G proteins from membrane to cytosol (23). Blockage of Rho is generally thought as the anticancer effect of statins. However, there are many evidences showing that nonlipid effect plays an important role in their anticancer activity (24, 25). To explore the

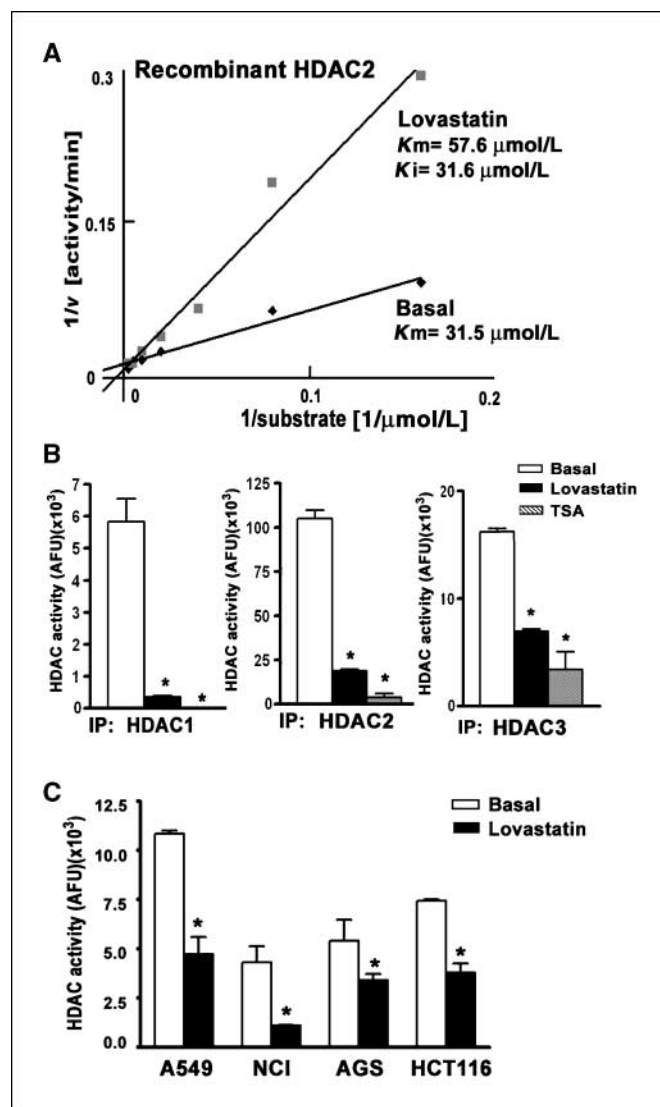


Figure 3. Inhibition of human recombinant HDAC2 activity by lovastatin. *A*, kinetic inhibition of human recombinant HDAC2 by lovastatin was determined in the presence of 6.75 to 200 μmol/L substrate using the HDAC activity assay kit as described in Materials and Methods, and the Lineweaver-Burk plot was presented. *B*, inhibition of HDAC1, HDAC2, or HDAC3 activity by 30 μmol/L lovastatin or 1 μmol/L TSA was determined. HDAC1, HDAC2, or HDAC3 was immunoprecipitated from A549 cells, and activity was determined using the HDAC activity assay kit as described in Materials and Methods. *Columns*, mean of three independent experiments performed in triplicate; *bars*, SE. *, *P* < 0.05 compared with basal. *C*, inhibition of HDAC activity in various cancer cells, including lung, gastric, and colon, by 30 μmol/L lovastatin was determined using HDAC activity assay kit as described in Materials and Methods. *Columns*, mean of three independent experiments performed in triplicate; *bars*, SE. *, *P* < 0.05 compared with basal.

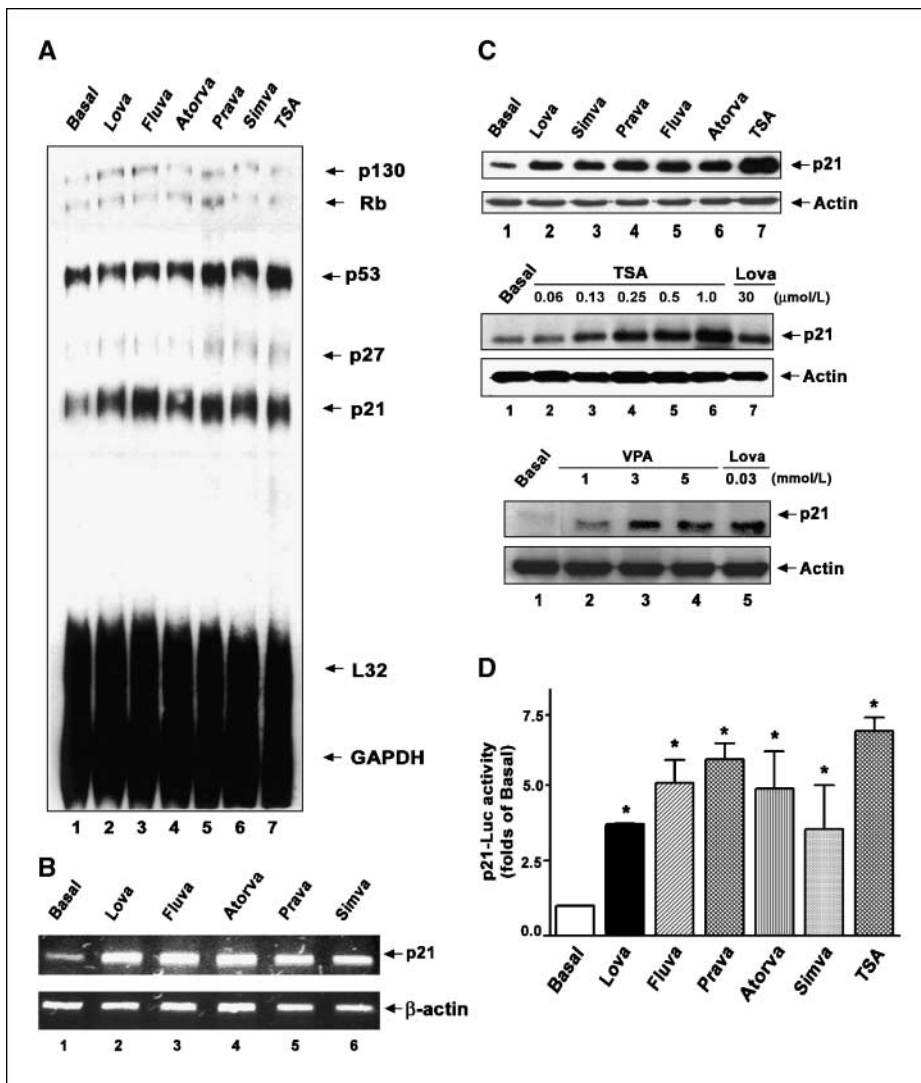


Figure 4. Statins increased the mRNA and protein expressions of p21. A549 cells were treated with 30 $\mu\text{mol/L}$ statins or 1 $\mu\text{mol/L}$ TSA for 16 h, then total mRNA were prepared and subjected to RPA, as described in Materials and Methods, and GAPDH and L32 were shown as internal controls (A) or mRNA was harvested and RT-PCR was performed (B). C, cells were treated with 30 $\mu\text{mol/L}$ statins or 1 $\mu\text{mol/L}$ TSA or different doses of TSA or VPA, then whole-cell lysates were prepared and subjected to Western blotting using antibody against p21 or actin. D, A549 cells were transfected with the luciferase reporter plasmid containing p21 promoter and then treated with 30 $\mu\text{mol/L}$ statins or 1 $\mu\text{mol/L}$ TSA. Luciferase activity was measured as described in Materials and Methods. Fold induction compared with the basal activity was expressed as the mean \pm SE of three independent experiments performed in triplicate. *, $P < 0.05$ compared with basal.

whole picture, we performed RPA to analyze the cell cycle-related genes and found that statins increased p21. RT-PCR and Western blot confirmed this up-regulation of p21. The role of HMG-CoA reductase is ruled out because mevalonate pretreatment cannot prevent p21 induction (data not shown).

A variety of transcription factors, such as p53, Sp1/Sp3, C/EBP α , and C/EBP β , have been reported to be critical for the p21 transcription in response to different stimulus. C/EBP α is required for the dexamethasone-induced transactivation of the p21 promoter. Antioxidants induce p21 expression through C/EBP β and sensitize the colon cancer cells to chemotherapy (26, 27). Foremost, p53 was considered as the most important regulator of p21 because there are two important p53-binding sites on the p21 promoter (28). The p21 transcription induced by some chemotherapeutic drugs or DNA damage has been reported to be p53 dependent (29, 30). IKK inhibitors α -methylene- γ -butyrolactone compounds can also induce p21 expression through up-regulation and acetylation of p53 (31).⁵ In contrast, statins-induced p21 expression is irrelevant to

p53, because promoter luciferase activity was not affected by p53 deletion and induction of p21 was still seen in HCT 116 p53^{-/-} cells. RPA results also showed no increase in p53 mRNA after statins treatment. The p53-independent induction of p21 expression is meaningful for the therapeutic value of statins, as loss or mutation of p53 is one of the most common defects observed in human cancers. These results imply that statins can circumvent the loss of wild-type p53 to induce cell cycle arrest through p21 induction.

The human p21 gene contains six Sp1 binding elements (Sp1-1 to Sp1-6) which play a major role in the regulation of p21 transcription (32). The transcription factor Sp1 is a member of Sp family that binds DNA through its COOH terminal zinc-finger motifs. Sp3 shares extensive structural and sequence homology with Sp1 and also binds to the Sp1 element on the promoters (28, 33). The Sp1 sites have been reported to be critical for p21 induction by HDAC inhibitors, such as TSA, SAHA, butyrate, and apicidin (34–37). To examine whether Sp1 element is involved in statin-induced p21 expression, p21 promoter constructs with different Sp1 mutation were used. The results showed the involvement of Sp1 in lovastatin-induced p21 promoter activity, and the major sites are Sp1-3 to Sp1-6. A model for regulation of p21 through recruitment of HDACs by Sp1/Sp3, which in turn represses p21 transcription in the resting

⁵ Y-C. Lin, unpublished data.

state has been reported (38). Supporting this hypothesis are some studies demonstrating that certain gene promoters are also repressed by HDACs through their Sp1 sites (39). In this study, the binding of Sp1/Sp3 to p21 promoter was not changed after treatment with lovastatin. We recently found the shift of CBP binding from p53 to p65 after nuclear activation of IKK α , which tips the balance for the transcriptional regulation of survival and apoptotic genes (40). This finding inspired us that the Sp1 switch from HDAC to CBP might exist to regulate p21 expression. DAPA and ChIP indeed reveal the recruitment of HDAC1 and HDAC2 to

the Sp1/Sp3 site in resting state, in which p21 expression was not seen. Lovastatin compels HDAC1/2 from p21 promoter and recruits CBP, resulting in histone-H3 acetylation. Although there are also reports demonstrating that SAHA release HDAC from Sp1 site on the p21 promoter (34), we are the first to show that statins decrease the binding of HDAC1/2 and recruit the binding of CBP to the p21 promoter. Similar to statins, antitumor agents farneyl-transferase inhibitors and geranylgeranyltransferase I inhibitors have also been found to up-regulate Rho expression through dissociation of HDAC and association of p300, leading to histone

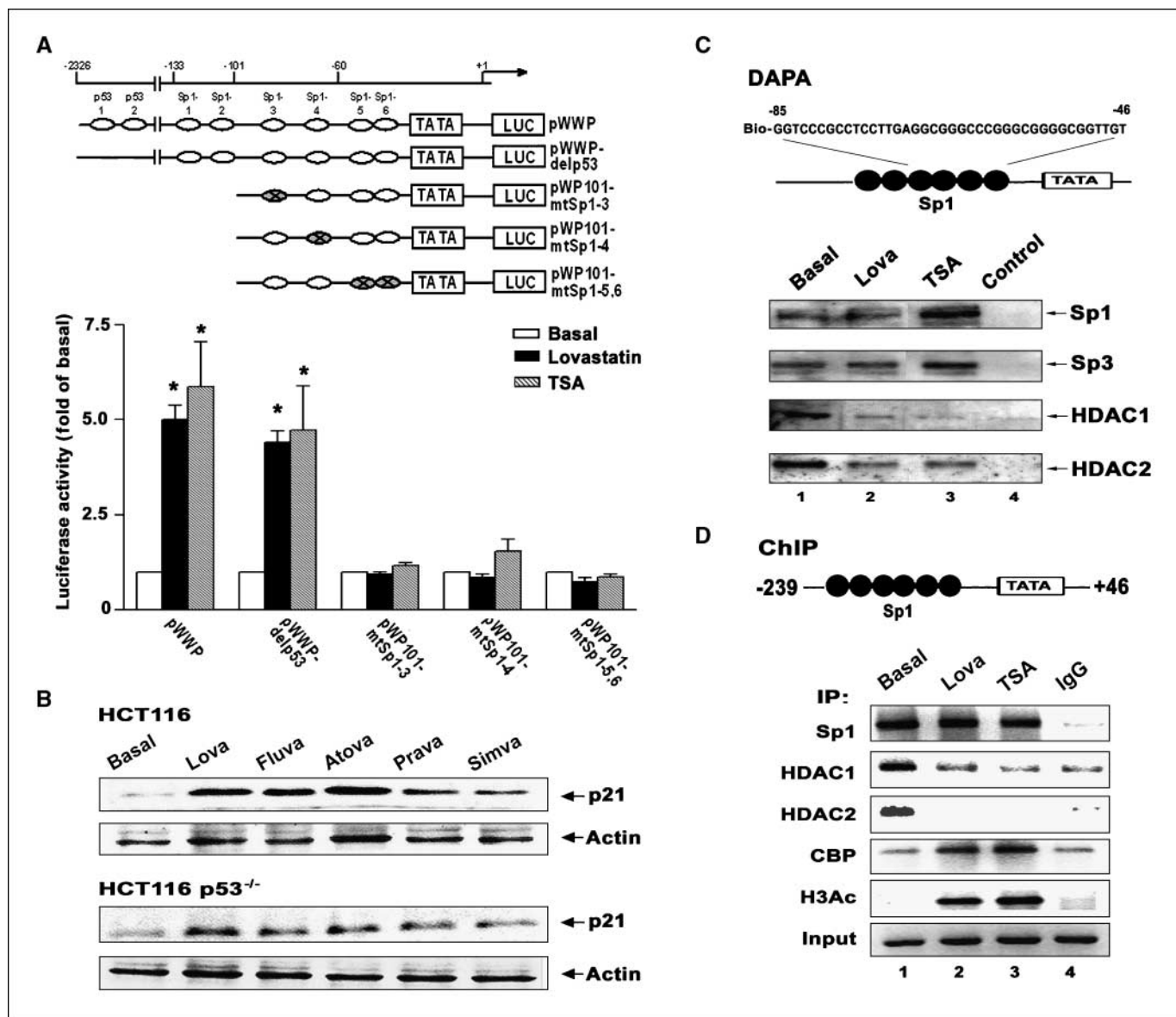


Figure 5. Involvement of Sp1 but not p53 in the statins-induced transcriptional activity of p21. *A*, top, schematic diagram of 5' regulatory region of human p21 gene. Circles, location of p53 and Sp1 sites; crosses, mutations within the Sp1 sites. A549 cells were transfected with various luciferase reporter plasmids and then treated with 30 μ mol/L lovastatin or 1 μ mol/L TSA for 16 h. Luciferase activity was measured as described in Materials and Methods. Fold induction compared with the basal activity was expressed as the mean \pm SE of three independent experiments performed in triplicate. *, $P < 0.05$ compared with basal. *B*, HCT116 (wild type) and HCT116 (p53^{-/-}) cells were treated with 30 μ mol/L statins for 16 h, and then whole-cell lysates were prepared and subjected to Western blotting using antibody against p21 or actin. *C* and *D*, A549 cells were treated with 30 μ mol/L lovastatin or 1 μ mol/L TSA for 16 h, and then nuclear extracts were prepared (C) or ChIP assay was performed (D). Nuclear extracts were mixed with biotinylated p21 promoter probe containing Sp1-3 to Sp1-6 sites, then Sp1, Sp3, HDAC1, or HDAC2 were detected by Western blotting, and result is a representative of three independent experiments (C). ChIP assays were performed using anti-Sp1, anti-HDAC1, anti-HDAC2, anti-CBP, or anti-acetylated histone-H3 (H3Ac) antibody or with rabbit nonimmune IgG (control). The precipitated p21 Sp1 region (+46 to -239) was assayed as described in Materials and Methods. Chromatin (1%) was assayed to verify equal loading (input). Results were falsely colored black for easier visualization (D).

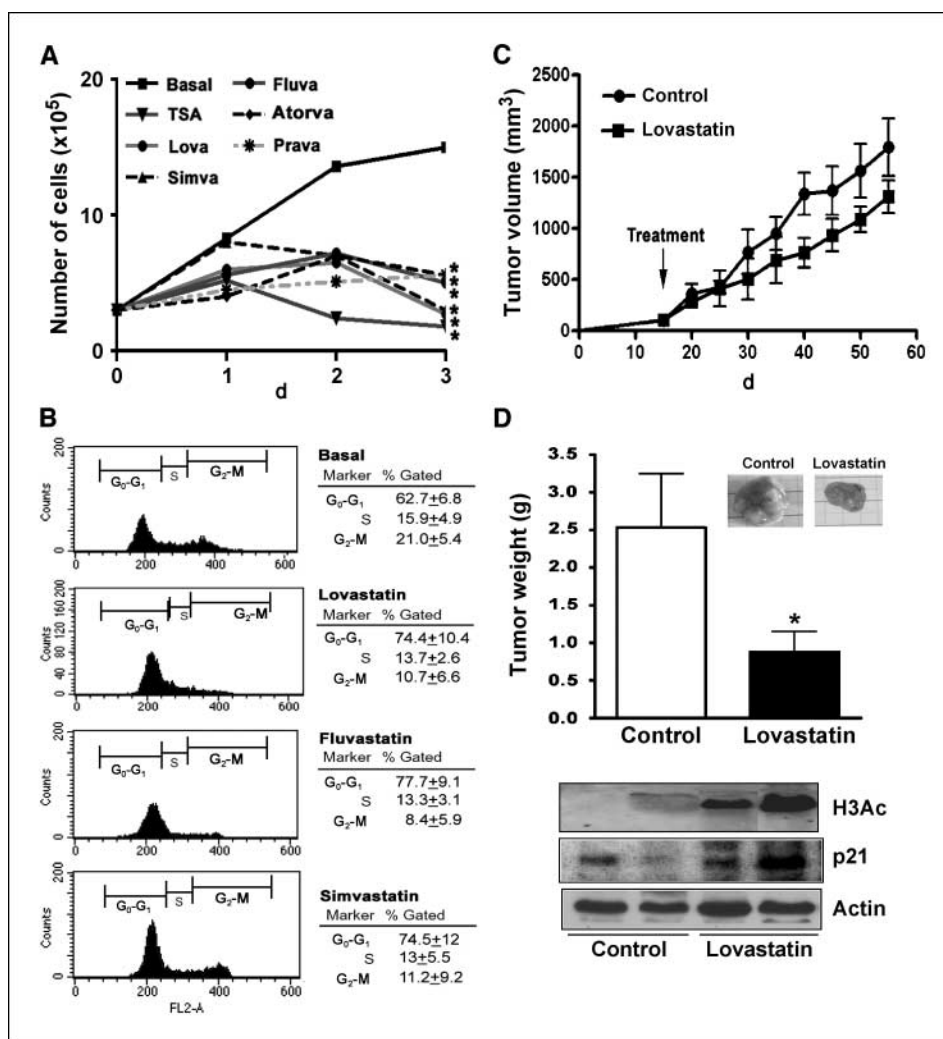


Figure 6. Inhibitory effect of statins on *in vitro* cell proliferation and *in vivo* tumor growth. **A**, cell growth of A549 cells treated with 10 $\mu\text{mol/L}$ statins or 0.5 $\mu\text{mol/L}$ TSA for 3 d was measured by MTT assay as described in Materials and Methods. Cell viability was compared with control cells (basal). **B**, A549 cells treated with 30 $\mu\text{mol/L}$ statins for 24 h were stained with propidium iodide, and G₀-G₁ fraction was analyzed by flow cytometer. **C**, A549 cells (10^6) were xenotransplanted into the right hip region of nude mice. After visible tumor formation, mice were randomly divided into two groups for p.o. treatment with lovastatin (20 mg/kg/d) or vehicle as described in Materials and Methods. The tumor volume was calculated as follows: $V = 0.52 \times (\text{width})^2 \times (\text{length})$. **D**, tumors were dissected and weighed. Photographs were tumors from vehicle-treated or lovastatin-treated mice. Protein lysates obtained from two randomly selected xenograft tumors were electrophoresed and immunoblotted with anti-p21, anti-H3Ac, or anti-actin antibody.

acetylation on the RhoB promoter (41). The incapability of HDACs to bind DNA directly means that HDACs are recruited indirectly to the promoter through associating with the Sp1 transcription factor. Coimmunoprecipitation experiments showed that PMA treatment shifted the binding of Sp1 from HDAC1 to coactivators p300, leading to the increase of histone-H3 acetylation on 12-(s)-lipoxygenase promoter and gene expression (42). The dissociation of HDAC and binding of p300/PCAF to the gene promoter other than p21 were only found in transforming growth factor- β type II receptor induced by TSA (43). Whether other known HDAC inhibitors or statins have similar effect remains to be determined.

Statins in acid form possess a carboxylic acid-containing aliphatic chain, a structure similar to the functional group of TSA and SAHA. We are the first to reveal that statins directly inhibit HDAC activity. Statins inhibited the HDAC activity in cancer cells but not in normal cells. Crystallographic studies have shown a zinc-dependent deacetylation catalyzed by HDLP (21). TSA mimicking the acetylated lysine has been shown to chelate the zinc in the catalytic pocket of HDLP by its hydroxamic acid (44). Our computational simulation revealed that TSA also nicely packs into the catalytic pocket of mammalian HDAC2 (Fig. 2A). Recent molecular dynamics simulations identified an additional pocket adjacent to the catalytic site that can modulate the HDAC2 conformations by accommodating the acetyl-lysine into the catalytic

site (45). According to the homology modeling and molecular docking, we found that lovastatin was able to bind both sites (Fig. 2B and C), suggesting that a composite butterfly compound that consists of two lovastatin molecules with a linker in-between might be able to bind HDAC2 even stronger than lovastatin does. Because the binding affinity of lovastatin to HDAC2 is already at the micromolar range, it is very likely that the composite butterfly compound could exhibit picomolar range affinity if the linker between the two lovastatin molecules is well designed. This novel binding mode to distinct inhibitor site also provides an additional opportunity for further drug development.

The HDAC inhibitor-induced increase in p21 expression seems to play a major role in arresting transformed cell growth. The relationship between HDAC inhibition and p21 transcription is based on the results that HDAC inhibitors release HDAC from p21 promoter and accumulate acetylation of the gene-associated histones (34). Differential groups of HDAC inhibitors with different K_i values, including TSA (0.28 nmol/L), VPA (0.5 mmol/L), or butyrate (2.25 mmol/L), have been found to induce p21 expression (46). The results were obtained from separate groups, and effects of these HDAC inhibitors were not compared simultaneously. In this study, we compared lovastatin ($K_i = 32 \mu\text{mol/L}$) with TSA and VPA. The global histone-H3 acetylation induced by 30 $\mu\text{mol/L}$ lovastatin is comparable with that induced by 0.5 $\mu\text{mol/L}$ TSA and 5 mmol/L

VPA, and so does p21 expression. Although the global histone-H3 acetylation induced by 1 $\mu\text{mol/L}$ TSA is much higher than 30 $\mu\text{mol/L}$ lovastatin, the extents of p21 induction and histone-H3 acetylation on p21 promoter are quite similar. DNA-bound histone-H3 acetylation is more accurate to reflect gene transcription, because global increase in acetylated histones is preferentially localized to the nuclear periphery that might not be associated to euchromatin (47).

In summary, statins represent a promising approach for cancer therapy. We proposed an "epigenetic mechanism" for statins. Compared with other HDAC inhibitors, statins is one of the best candidates for chemoprevention, because the clinical application

has been well characterized and side effects seem to be less than the known HDAC inhibitors.

Acknowledgments

Received 10/11/2007; revised 1/2/2008; accepted 1/17/2008.

Grant support: National Science Council of Taiwan grant NSC-96-2320-B002 and Frontier and Innovative Research of National Taiwan University to C-C Chen. J-H. Lin was supported by Research Center for Applied Sciences, Academia Sinica. This work is partially supported by the National Science Council of Taiwan for funding awarded to J-H. Lin under the contract 95-2627-B-002-010.

The costs of publication of this article were defrayed in part by the payment of page charges. This article must therefore be hereby marked *advertisement* in accordance with 18 U.S.C. Section 1734 solely to indicate this fact.

References

- Pedersen TR, Wilhelmsen L, Faergeman O, et al. Follow-up study of patients randomized in the Scandinavian simvastatin survival study (4S) of cholesterol lowering. *Am J Cardiol* 2000;86:257-62.
- Yoshioka K, Nakamori S, Itoh K. Overexpression of small GTP-binding protein RhoA promotes invasion of tumor cells. *Cancer Res* 1999;59:2004-10.
- Hawk E, Viner JL. Statins and cancer-beyond the "one drug, one disease" model. *N Engl J Med* 2005;352:2238-9.
- Danesh FR, Sadeghi MM, Amro N, et al. 3-Hydroxy-3-methylglutaryl CoA reductase inhibitors prevent high glucose-induced proliferation of mesangial cells via modulation of Rho GTPase/p21 signaling pathway: implications for diabetic nephropathy. *Proc Natl Acad Sci U S A* 2002;99:8301-5.
- Lee SJ, Ha MJ, Lee J, et al. Inhibition of the 3-hydroxy-3-methylglutaryl-coenzyme A reductase pathway induces p53-independent transcriptional regulation of p21(WAF1/CIP1) in human prostate carcinoma cells. *J Biol Chem* 1998;273:10618-23.
- Jenuwein T, Allis CD. Translating the histone code. *Science* 2001;293:1074-80.
- Fraga MF, Ballestar E, Villar-Garea A, et al. Loss of acetylation at Lys16 and trimethylation at Lys20 of histone H4 is a common hallmark of human cancer. *Nat Genet* 2005;37:391-400.
- Bolden JE, Peart MJ, Johnstone RW. Anticancer activities of histone deacetylase inhibitors. *Nat Rev Drug Discov* 2006;5:769-84.
- Lin RJ, Evans RM. Acquisition of oncogenic potential by RAR chimeras in acute promyelocytic leukemia through formation of homodimers. *Mol Cell* 2000;5:821-30.
- Minucci S, Pelicci PG. Histone deacetylase inhibitors and the promise of epigenetic (and more) treatments for cancer. *Nat Rev Cancer* 2006;6:38-51.
- Thompson JD, Higgins DG, Gibson TJ. CLUSTAL W: improving the sensitivity of progressive multiple sequence alignment through sequence weighting, position-specific gap penalties and weight matrix choice. *Nucleic Acids Res* 1994;22:4673-80.
- Sali A, Blundell TL. Comparative protein modelling by satisfaction of spatial restraints. *J Mol Biol* 1993;234:779-815.
- Laskowski RA, MacArthur MW, Moss DS, Thornton JM. PROCHECK: a program to check the stereochemical quality of protein structures. *J Appl Crystallog* 1993;26:283-91.
- Morris AL, MacArthur MW, Hutchinson EG, Thornton JM. Stereochemical quality of protein structure coordinates. *Proteins* 1992;12:345-64.
- Li H, Robertson AD, Jensen JH. Very fast empirical prediction and rationalization of protein pKa values. *Proteins* 2005;61:704-21.
- Dolinsky TJ, Nielsen JE, McCammon JA, Baker NA. PDB2PQR: an automated pipeline for the setup of Poisson-Boltzmann electrostatics calculations. *Nucleic Acids Res* 2004;32:W665-7.
- Morris G, Goodsell D, Halliday R, et al. Automated docking using a Lamarckian genetic algorithm and an empirical binding free energy function. *J Comp Chem* 1998;19:1639-62.
- Chang DT, Oyang YJ, Lin JH. MEDock: a web server for efficient prediction of ligand binding sites based on a novel optimization algorithm. *Nucleic Acids Res* 2005;33:W233-8.
- Stote RH, Karplus M. Zinc binding in proteins and solution: a simple but accurate nonbonded representation. *Proteins* 1995;23:12-31.
- Lin YC, Shun CT, Wu MS, Chen CC. A novel anticancer effect of thalidomide: inhibition of intercellular adhesion molecule-1-mediated cell invasion and metastasis through suppression of nuclear factor- κ B. *Clin Cancer Res* 2006;12:7165-73.
- Finnin MS, Donigian JR, Cohen A, et al. Structures of a histone deacetylase homologue bound to the TSA and SAHA inhibitors. *Nature* 1999;401:188-93.
- Demieire MF, Higgins PD, Gruber SB, Hawk E, Lippman SM. Statins and cancer prevention. *Nat Rev Cancer* 2005;5:930-42.
- Mo H, Elson CE. Studies of the isoprenoid-mediated inhibition of mevalonate synthesis applied to cancer chemotherapy and chemoprevention. *Exp Biol Med (Maywood)* 2004;229:567-85.
- Nubel T, Dippold W, Kleintert H, Kaina B, Fritz G. Lovastatin inhibits Rho-regulated expression of E-selectin by TNF α and attenuates tumor cell adhesion. *FASEB J* 2004;18:140-2.
- Wong WW, Dimitroulakos J, Minden MD, Penn LZ. HMG-CoA reductase inhibitors and the malignant cell: the statin family of drugs as triggers of tumor-specific apoptosis. *Leukemia* 2002;16:508-19.
- Cram EJ, Ramos RA, Wang EC, Cha HH, Nishio Y, Firestone GL. Role of the CCAAT/enhancer binding protein- α transcription factor in the glucocorticoid stimulation of p21waf1/cip1 gene promoter activity in growth-arrested rat hepatoma cells. *J Biol Chem* 1998;273:2008-14.
- Chinery R, Brockman JA, Peeler MO, Shyr Y, Beauchamp RD, Coffey RJ. Antioxidants enhance the cytotoxicity of chemotherapeutic agents in colorectal cancer: a p53-independent induction of p21WAF1/CIP1 via C/EBP β . *Nat Med* 1997;3:1233-41.
- Kagawa S, Fujiwara T, Hizuta A, et al. p53 expression overcomes p21WAF1/CIP1-mediated G1 arrest and induces apoptosis in human cancer cells. *Oncogene* 1997;15:1903-9.
- MacLeod KF, Sherry N, Hannon G, et al. p53-dependent and independent expression of p21 during cell growth, differentiation, and DNA damage. *Genes Dev* 1995;9:935-44.
- el-Deiry WS, Tokino T, Velculescu VE, et al. WAF1, a potential mediator of p53 tumor suppression. *Cell* 1993;75:817-25.
- Huang WC, Chan ST, Yang TL, Tzeng CC, Chen CC. Inhibition of ICAM-1 gene expression, monocyte adhesion and cancer cell invasion by targeting IKK complex: molecular and functional study of novel α -methylene- γ -butyrolactone derivatives. *Carcinogenesis* 2004;25:1925-34.
- Gartel AL, Tyner AL. Transcriptional regulation of the p21(WAF1/CIP1) gene. *Exp Cell Res* 1999;246:280-9.
- Sowa Y, Orita T, Minamikawa-Hiranabe S, Mizuno T, Nomura H, Sakai T. Sp3, but not Sp1, mediates the transcriptional activation of the p21/WAF1/Cip1 gene promoter by histone deacetylase inhibitor. *Cancer Res* 1999;59:4266-70.
- Gui CY, Ngo L, Xu WS, Richon VM, Marks PA. Histone deacetylase (HDAC) inhibitor activation of p21WAF1 involves changes in promoter-associated proteins, including HDAC1. *Proc Natl Acad Sci U S A* 2004;101:1241-6.
- Sowa Y, Orita T, Minamikawa S, et al. Histone deacetylase inhibitor activates the WAF1/Cip1 gene promoter through the Sp1 sites. *Biochem Biophys Res Commun* 1997;241:142-50.
- Rocchi P, Tonelli R, Camerin C, et al. p21Waf1/Cip1 is a common target induced by short-chain fatty acid HDAC inhibitors (valproic acid, tributyrin and sodium butyrate) in neuroblastoma cells. *Oncol Rep* 2005;13:1139-44.
- Han JW, Ahn SH, Park SH, et al. Apicidin, a histone deacetylase inhibitor, inhibits proliferation of tumor cells via induction of p21WAF1/Cip1 and gelsolin. *Cancer Res* 2000;60:6068-74.
- Varshochi R, Halim F, Sunters A, et al. ICI182,780 induces p21Waf1 gene transcription through releasing histone deacetylase 1 and estrogen receptor α from Sp1 sites to induce cell cycle arrest in MCF-7 breast cancer cell line. *J Biol Chem* 2005;280:3185-96.
- Yokota T, Matsuzaki Y, Miyazawa K, Zindy F, Roussel MF, Sakai T. Histone deacetylase inhibitors activate INK4d gene through Sp1 site in its promoter. *Oncogene* 2004;23:5340-9.
- Huang WC, Ju TK, Hung MC, Chen CC. Phosphorylation of CBP by IKK α promotes cell growth by switching the binding preference of CBP from p53 to NF- κ B. *Mol Cell* 2007;26:75-87.
- Delarue FL, Adnane J, Joshi B, et al. Farnesyltransferase and geranylgeranyltransferase I inhibitors upregulate RhoB expression by HDAC1 dissociation, HAT association and histone acetylation of the RhoB promoter. *Oncogene* 2007;26:633-40.
- Hung JJ, Wang YT, Chang WC. Sp1 deacetylation induced by phorbol ester recruits p300 to activate 12(S)-lipoxygenase gene transcription. *Mol Cell Biol* 2006;26:1770-85.
- Huang W, Zhao S, Ammanamanchi S, Brattain M, Venkatasubbarao K, Freeman JW. Trichostatin A induces transforming growth factor β type II receptor promoter activity and acetylation of Sp1 by recruitment of PCAF/p300 to a Sp1.NF-Y complex. *J Biol Chem* 2005;280:10047-54.
- Vanommeslaeghe K, Van AC, De PF, Martins JC, Tourwe D, Geerlings P. Ab initio study of the binding of Trichostatin A (TSA) in the active site of histone deacetylase like protein (HDLP). *Org Biomol Chem* 2003;1:2951-7.
- Wang DF, Helquist P, Wiech NL, Wiest O. Toward selective histone deacetylase inhibitor design: homology modeling, docking studies, and molecular dynamics simulations of human class I histone deacetylases. *J Med Chem* 2005;48:6936-47.
- Eyal S, Yagen B, Sobol E, Altschuler Y, Shmuel M, Bialer M. The activity of antiepileptic drugs as histone deacetylase inhibitors. *Epilepsia* 2004;45:737-44.
- Rada-Iglesias A, Enroth S, Ameer A, et al. Butyrate mediates decrease of histone acetylation centered on transcription start sites and down-regulation of associated genes. *Genome Res* 2007;17:708-19.